

Topological superfluidity of lattice fermions inside a Bose-Einstein condensate

Jonatan Melkær Midtgaard,¹ Zhiqiang Wu,¹ and G. M. Bruun¹

¹*Department of Physics and Astronomy, Aarhus University, Ny Munkegade, DK-8000 Aarhus C, Denmark*
(Dated: September 22, 2018)

We calculate the phase diagram of identical fermions in a 2-dimensional (2D) lattice immersed in a 3D Bose-Einstein condensate (BEC). The fermions exchange density fluctuations in the BEC, which gives rise to an attractive induced interaction. The resulting zero temperature phase diagram exhibits topological $p_x + ip_y$ superfluid phases as well as a phase separation region. We show how to use the flexibility of the Bose-Fermi mixture to tune the induced interaction, so that it maximises the pairing between nearest neighbour sites, whereas phase separation originating from long range interactions is suppressed. Finally, we calculate the Berezinskii-Kosterlitz-Thouless (BKT) critical temperature of the topological superfluid in the lattice and discuss experimental realisations.

I. INTRODUCTION

Ever since topological superfluids/superconductors with Majorana modes were predicted to exist [1], it has been a major research goal to detect them. Experimental evidence for Majorana modes have been reported in 1D wires [2–8], and Sr_2RuO_4 is a promising candidate for realising a 2D topological superconductor [9–12]. An unambiguous detection of topological superconductivity/superfluidity is however still lacking, partly due to the complexity of these condensed matter systems. There are several proposals to use the clean and highly flexible atomic quantum gases to overcome this difficulty. The first scheme was based on Fermi gases interacting via a p -wave Feshbach resonance [13], but these systems suffer from short lifetimes [14–17]. Other quantum gas proposals include schemes based on optical lattices [18–21], synthetic spin-orbit coupling [22–24], driven dissipation [25, 26], dipolar molecules [27–29], and mixed dimension Fermi-Fermi mixtures [30]. Unfortunately, none of these systems have been realised so far.

Very recently, two of us (ZW and GMB) demonstrated that a mixed dimension Fermi-Bose mixture constitutes a promising system to realise a 2D topological superfluid [31]. In this proposal, identical fermions are confined in a 2D plane and they interact via density modulations in a surrounding BEC. Due to the high compressibility of the BEC, this induced interaction is strong, and one can moreover control the range by varying the BEC coherence length. This flexibility can be used to make the critical temperature of the topological superfluid high, while keeping three-body losses small. The purpose of the present paper is to examine this promising scheme in a setup, where the fermions are moving in a 2D optical lattice. Optical lattices offer the particular advantage of single site resolution spectroscopy [32, 33], which presents unique opportunities to detect and manipulate Majorana edge modes [34, 35]. We therefore investigate the phase diagram of identical fermions moving in a 2D square lattice immersed in a 3D BEC, which gives rise to an attractive induced interaction between the fermions. As a result, the ground state of the fermions is a topological $p_x + ip_y$ superfluid, but the system also suffers

from a phase separation instability originating from an underlying particle-hole symmetry in the lattice. Taking the competition of these two instabilities into account, we calculate the zero temperature phase diagram of the fermions as a function of the Bose-Fermi coupling strength and the filling fraction. We show how to use the flexibility of the Bose-Fermi system to tune the interaction in order to maximise the pairing strength, while keeping the system stable against phase separation. The key point to solve this delicate problem turns out to be to adjust the range of the interaction by changing the BEC coherence length, so that it induces pairing on neighboring sites, while it does not lead to a significant long range interaction effects beyond nearest neighbors. We finally calculate the BKT critical temperature for the superfluid phase and discuss experimental realisations.

II. MODEL

We consider fermionic atoms of mass m moving in a 2D square lattice in the xy -plane. The lattice is immersed in a 3D BEC consisting of atoms with mass m_B , which is weakly interacting with $n_0 a_B^3 \ll 1$, so that it can be accurately described by Bogoliubov theory. Here n_0 denotes the condensate density and a_B the boson-boson scattering length. The setup is illustrated in Fig. 1. The Hamiltonian is

$$H = -t \sum_{\langle i,j \rangle} (a_i^\dagger a_j + \text{h.c.}) + \sum_{\mathbf{k}} E_{\mathbf{k}} \gamma_{\mathbf{k}}^\dagger \gamma_{\mathbf{k}} + H_{\text{int}}, \quad (1)$$

where t is the hopping matrix element of the fermions between nearest neighbor sites $\langle i, j \rangle$, a_i^\dagger creates a fermion at lattice site i , and $\gamma_{\mathbf{k}}^\dagger$ creates a Bogoliubov mode in the BEC with momentum \mathbf{k} and energy $E_{\mathbf{k}} = [\epsilon_{\mathbf{k}}^B (\epsilon_{\mathbf{k}}^B + 8\pi n_0 a_B / m_B)]^{1/2}$ where $\epsilon_{\mathbf{k}}^B = k^2 / 2m_B$. We use units for which $k_B = \hbar = 1$. Within the pseudopotential approximation, the interaction between the fermions and the bosons is

$$H_{\text{int}} = g \int d^3r \psi_F^\dagger(\mathbf{r}) \psi_B^\dagger(\mathbf{r}) \psi_B(\mathbf{r}) \psi_F(\mathbf{r}), \quad (2)$$

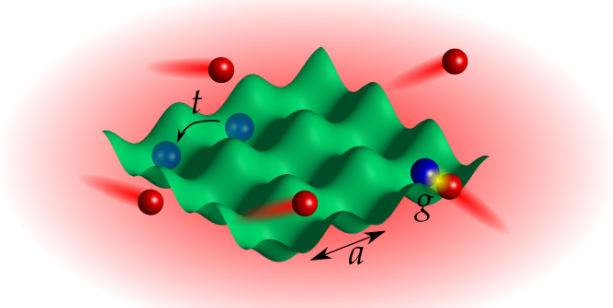


FIG. 1. (Color online). Illustration of the mixed-dimensional system. The fermions (blue balls) move in a 2D square lattice in the xy -plane with lattice constant a and hopping matrix element t . The lattice is immersed in a 3D BEC (red balls) and the fermions and bosons interact through a contact interaction with strength g .

where $\psi_B(\mathbf{r})$ and $\psi_F(\mathbf{r})$ is the field operator for the bosons and fermions respectively. The coupling strength is $g = 2\pi a/m_r$, with a the Bose-Fermi scattering length and $m_r = mm_B/(m + m_B)$ the reduced mass. For a deep optical lattice, the fermion field operator can be approximated by $\psi_F(\mathbf{r}) = \sum_i \phi_0(\mathbf{r} - \mathbf{r}_i) a_i$ where $\phi_0(\mathbf{r} - \mathbf{r}_i)$ is the lowest Wannier function for site i located at \mathbf{r}_i . We approximate the Wannier function by a Gaussian $\phi_0(\mathbf{r}) = \exp(-r_\perp^2/2\ell_\perp^2 - z^2/2\ell_z^2)/\pi^{3/4}\ell_\perp\sqrt{\ell_z}$ where $\mathbf{r}_\perp = (x, y)$ is a vector in the lattice plane, and ℓ_z and ℓ_\perp are the oscillator lengths of the potential wells of the 2D lattice perpendicular and parallel to the plane. Using this in Eq. (1), we obtain

$$H_{\text{int}} = \frac{g}{\mathcal{V}} \sum_{i, \mathbf{k}, \mathbf{q}} e^{-\frac{1}{4}\ell_z^2 q_z^2} e^{-\frac{1}{4}\ell_\perp^2 q_\perp^2} e^{-i\mathbf{q}_\perp \cdot \mathbf{r}_i} b_{\mathbf{k}+\mathbf{q}}^\dagger b_{\mathbf{k}} a_i^\dagger a_i \quad (3)$$

for the Bose-Fermi interaction, where \mathcal{V} is the system volume and $b_{\mathbf{k}}^\dagger$ creates a boson with momentum \mathbf{k} . We have the usual Bogoliubov relation $b_{\mathbf{k}} = u_{\mathbf{k}}\gamma_{\mathbf{k}} - v_{\mathbf{k}}\gamma_{-\mathbf{k}}^\dagger$ with $u_{\mathbf{k}}^2 = [1 + (\epsilon_{\mathbf{k}}^B + 4\pi n_0 a_B)/E_{\mathbf{k}}]/2$ and $v_{\mathbf{k}}^2 = [-1 + (\epsilon_{\mathbf{k}}^B + 4\pi n_0 a_B)/E_{\mathbf{k}}]/2$.

III. EFFECTIVE HAMILTONIAN FOR THE FERMIONS

Since the bosons live in 3D whereas the fermions are confined to a 2D lattice, we expect the BEC to be essentially unaffected by the fermions. On the other hand, the fermions interact with each other via the bosons and we will in this section derive an effective Hamiltonian describing this. One fermion will either attract or repel the bosons thereby changing the local density of the BEC, which is felt by the second fermion. This results in the

induced interaction

$$V_{\text{ind}}(i, j, i\omega_q) = g^2 \int \frac{d^3q}{(2\pi)^3} e^{i\mathbf{q}_\perp \cdot (\mathbf{r}_i - \mathbf{r}_j)} e^{-(\ell_z^2 q_z^2 - \ell_\perp^2 q_\perp^2)/2} \times \chi_B(\mathbf{q}, i\omega_q) \quad (4)$$

between the fermions, where $\mathbf{q}_\perp = (q_x, q_y)$ is a 2D momentum, $\mathbf{q} = (q_x, q_y, q_z)$ is a 3D momentum, and $i\omega_q$ is a bosonic Matsubara frequency. The density-density correlation function of the BEC is

$$\chi_B(\mathbf{q}, i\omega_q) = \frac{q^2}{m_B} \frac{n_0}{(i\omega_q)^2 - E_{\mathbf{q}}^2}. \quad (5)$$

Equation (4) includes an integration over the z component q_z of the boson momentum, since this is not conserved by the Bose-Fermi interaction given by Eq. (3).

For simplicity, we take the limit $\ell_\perp \rightarrow 0$ and $\ell_z \rightarrow 0$ in the following. We furthermore assume that the speed of sound $c_s = \sqrt{4\pi a_B n_0}/m_B$ in the BEC is much larger than ta , where a is the lattice constant. This means that retardation effects are negligible so that the frequency can be set to zero in the induced interaction. When c_s becomes comparable to ta , we expect retardation effects to significantly suppress pairing in analogy with what happens for the corresponding system without a lattice [31]. Ignoring retardation effects by setting $i\omega_q = 0$ in Eq. (4) yields the usual Yukawa interaction [36, 37]

$$V_{\text{ind}}(i, j) = -g^2 \frac{n_0 m_B}{\pi} \frac{e^{-\sqrt{2}|\mathbf{r}_i - \mathbf{r}_j|/\xi_B}}{|\mathbf{r}_i - \mathbf{r}_j|}, \quad (6)$$

where $\xi_B = (8\pi a_B n_0)^{-1/2}$ is the BEC coherence length. It follows from Eq. (6) that the dimensionless parameter determining the strength of the induced interaction between the fermions in the lattice is

$$G = \frac{g^2 n_0 m_B}{\pi a t}. \quad (7)$$

Equation (6) illustrates another important fact: By varying the Bose density n_0 and/or the scattering lengths a_B and a_I , one can experimentally control both the *strength* as well as the *range* (determined by ξ_B) of the induced interaction between the fermions.

Using the induced interaction, the effective Hamiltonian for the fermions is

$$H_{\text{eff}} = -t \sum_{\langle i, j \rangle} a_i^\dagger a_j - \mu \sum_j a_j^\dagger a_j + \sum_{i < j} V_{\text{ind}}(i, j) a_i^\dagger a_j^\dagger a_j a_i, \quad (8)$$

where $V_{\text{ind}}(i, j)$ is given by Eq. (6) and we have subtracted the chemical potential μ as usual. Note that the system is symmetric under the particle-hole transformation $\mathcal{P} a_i \mathcal{P}^{-1} = a_i^\dagger$, where the filling fraction transforms as $n \rightarrow 1 - n$, the hopping matrix element as $t \rightarrow -t$, and the chemical potential as $\mu \rightarrow -\mu + \sum_j V_{\text{ind}}(0, j)$.

IV. ZERO TEMPERATURE PHASE DIAGRAM

Using the effective Hamiltonian given by Eq. (8), we will now calculate the $T = 0$ phase diagram of the fermions in the lattice. We shall consider two possible instabilities of the system caused by the induced interaction: A superfluid and a phase separation instability. To do this, we decouple the interaction in the Hartree-Fock and BCS channels. Assuming pairing between \mathbf{k} and $-\mathbf{k}$ states, the mean-field Hamiltonian becomes (apart from a constant)

$$H_{\text{MF}} = \frac{1}{2} \sum_{\mathbf{k}} [a_{\mathbf{k}}^\dagger \ a_{-\mathbf{k}}] \begin{bmatrix} \xi_{\mathbf{k}} & \Delta_{\mathbf{k}} \\ \Delta_{\mathbf{k}}^* & -\xi_{\mathbf{k}} \end{bmatrix} \begin{bmatrix} a_{\mathbf{k}} \\ a_{-\mathbf{k}}^\dagger \end{bmatrix}, \quad (9)$$

where $\xi_{\mathbf{k}} = \epsilon_{\mathbf{k}} + \Sigma_{\mathbf{k}} - \mu$. Here, $\epsilon_{\mathbf{k}} = -2t(\cos k_x a + \cos k_y a)$ is the kinetic energy dispersion of the 2D lattice and

$$\Sigma_{\mathbf{k}} = \frac{1}{2\mathcal{V}} \sum_{\mathbf{k}'} [V_{\text{ind}}(0) - V_{\text{ind}}(\mathbf{k} - \mathbf{k}')] \times \left[1 - \frac{\xi_{\mathbf{k}'}}{E_{\mathbf{k}'}} \tanh\left(\frac{E_{\mathbf{k}'}}{2T}\right) \right] \quad (10)$$

is the Hartree-Fock self-energy. The Fourier transform $V_{\text{ind}}(\mathbf{k})$ is given by

$$V_{\text{ind}}(\mathbf{k}) = \frac{1}{N} \sum_{i \neq 0} V_{\text{ind}}(0, i) e^{i\mathbf{k} \cdot \mathbf{r}_i}, \quad (11)$$

where N is the number of lattice sites. The quasiparticle dispersion is $E_{\mathbf{k}} = (\xi_{\mathbf{k}}^2 + |\Delta_{\mathbf{k}}|^2)^{1/2}$ with the gap parameter determined by

$$\Delta_{\mathbf{k}} = -\frac{1}{2\mathcal{V}} \sum_{\mathbf{k}'} V_{\text{ind}}(\mathbf{k} - \mathbf{k}') \frac{\Delta_{\mathbf{k}'}}{E_{\mathbf{k}'}} \tanh\left(\frac{E_{\mathbf{k}'}}{2T}\right). \quad (12)$$

As usual, we solve Eqs. (10) and (12) self-consistently together with the number equation

$$n = \frac{1}{2} \left[1 - \frac{1}{N} \sum_{\mathbf{k}} \frac{\xi_{\mathbf{k}}}{E_{\mathbf{k}}} \tanh\left(\frac{E_{\mathbf{k}}}{2T}\right) \right], \quad (13)$$

which gives the filling fraction $0 \leq n \leq 1$ of the lattice. Our numerical calculations are performed on a $N = 121 \times 121$ lattice of \mathbf{k} -values in the first Brillouin zone.

A. Topological $p_x + ip_y$ superfluid

At zero temperature, we find a solution characterised by a gap with $p_x + ip_y$ symmetry. Indeed, the gap is very close to the pure $l = 1$ angular momentum form $\Delta_{\mathbf{k}} \propto \sin k_x a + i \sin k_y a$ as illustrated in Fig. 2. This solution is the most stable energetically, as it fully gaps the Fermi surface, in contrast to for instance a solution with p_x symmetry [38]. The $p_x + ip_y$ pairing breaks time-reversal

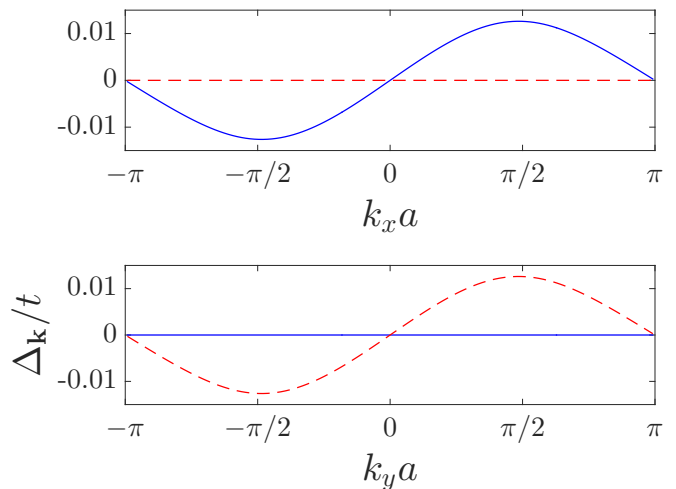


FIG. 2. The gap parameter $\Delta_{\mathbf{k}}$ as a function of momentum \mathbf{k} for the coupling strength $G = 3$, BEC coherence length $\xi_B/a = 1$, and filling fraction $n = 0.2$. The solid (blue) line shows the real part of the gap parameter, while the dashed (red) line shows the imaginary part. In the upper figure, we have taken $k_y = 0$ and in the lower we have taken $k_x = 0$.

symmetry and it is a class D topological superfluid with Majorana modes at its edges [39–42]. The topological invariant is the Chern number

$$\nu = \frac{1}{4\pi} \int_{\text{BZ}} d^2k [\hat{\mathbf{s}}(\mathbf{k}) \cdot (\partial_{k_x} \hat{\mathbf{s}}(\mathbf{k}) \times \partial_{k_y} \hat{\mathbf{s}}(\mathbf{k}))], \quad (14)$$

where $\hat{\mathbf{s}}(\mathbf{k}) = \mathbf{S}(\mathbf{k})/|\mathbf{S}(\mathbf{k})|$. Here $\mathbf{S}(\mathbf{k})$ is defined as usual by writing the BCS Hamiltonian as $\begin{bmatrix} \xi_{\mathbf{k}} & \Delta_{\mathbf{k}} \\ \Delta_{\mathbf{k}}^* & -\xi_{\mathbf{k}} \end{bmatrix} = \mathbf{S}(\mathbf{k}) \cdot \sigma$, with $\sigma = (\sigma_x, \sigma_y, \sigma_z)$ the vector of Dirac spin 1/2 matrices. For our model, the Chern number is $\nu = -1$ for a filling fraction $0 < n < 1/2$ and $\nu = 1$ for $1/2 < n < 1$. There is therefore a topological phase transition at half filling, $n = 1/2$, where the spectral gap closes at the points $(k_x, k_y) = (0, \pm\pi/a)$ and $(k_x, k_y) = (\pm\pi/a, 0)$ in the Brillouin zone.

B. Phase separation

The system becomes unstable towards phase separation when the induced interaction between the fermions is too attractive, which originates from the underlying particle-hole symmetry due to the lattice. The instability arises from the compressibility $\kappa = n^{-2} \partial_\mu n$ being negative for certain filling fractions. As an example, we plot in Fig. 3 the chemical potential μ as a function of filling fraction n for coupling strength $G = 3$, range $\xi_B/a = 1$, and temperatures $T = 0$, $T = 0.3t$, and $T = 0.6t$. For $T = 0$ and $T = 0.3t$, we see that μ decreases with n for a range of filling fractions, which corresponds to a negative compressibility, signalling that the system is unstable towards phase separation. The region of phase separation can be determined by the Maxwell construction. Due to

the particle-hole symmetry, this simplifies into the condition that a system with average filling fraction n phase separates into regions with filling fractions $n_1 < n$ and $n_2 = 1 - n_1 > n$ determined by $\mu(n_1) = \mu(1/2) = \mu(n_2)$. The resulting range of filling fractions where the system phase separates, is shown in Fig. 3 for $T = 0$. We also see from Fig. 3 that this range shrinks with increasing temperature. Indeed, the system does not separate at all for $T = 0.6t$. The reason is that the entropy of mixing stabilises the system against phase separation for a non-zero temperature.

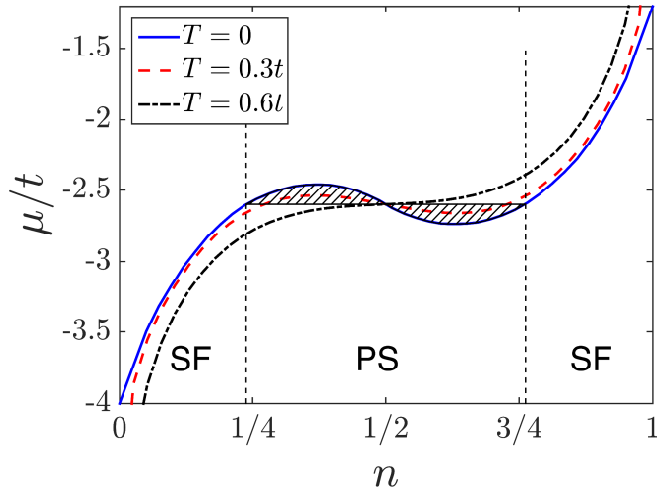


FIG. 3. Plot of the chemical potential μ as a function of filling fraction n for $G = 3$, $\xi_B/a = 1$, and different temperatures. The solid (blue) curve for $T = 0$ has the Maxwell construction indicated, where the system is unstable towards phase separation for the filling fractions between the vertical dashed lines, and superfluid outside that region. The dashed (red) curve for $T = 0.3t$ and the dot-dashed (black) curve for $T = 0.6t$ show how the phase separation region shrinks and finally disappears with increasing temperature.

C. Phase diagrams

We now present $T = 0$ phase diagrams taking the pairing and phase separation instabilities into account. In Fig. 4, we plot phase diagrams as a function of the filling fraction n and the Bose-Fermi coupling strength G for two different values of the BEC coherence length: $\xi_B/a = 1$ and $\xi_B/a = 1/2$. The system is phase separated in the gray regions, whereas it is in the $p_x + ip_y$ superfluid state in the other regions with the color code indicating the maximum value of $|\Delta_{\mathbf{k}}|$ in the Brillouin zone. The vertical line at half filling indicates a topological phase transition between a superfluid state with Chern number $\nu = -1$ and $\nu = 1$. As expected, an increasing coupling strength G increases the pairing. However, it also increases the range of densities where the system phase separates. Because of this competition, it is not simply a matter of increasing G in order to in-

crease the pairing. If the attraction becomes too strong, the system simply phase separates into regions with filling fractions close to $n = 0$ and $n = 1$, which strongly suppresses pairing. Instead, one has to tune G to an intermediate value to optimise the pairing. For a given G , one should choose an average filling fraction n in the phase separated region, i.e. $n_1 \leq n \leq 1 - n_1$. The system will then phase separate into two superfluid regions with filling fractions n_1 and $1 - n_1$, which have the same pairing strength. An important conclusion from Fig. 4 is that a smaller coherence length ξ_B allows one to obtain a larger pairing strength by tuning (n, G) . Indeed, the maximum value of the pairing one can achieve by tuning (n, G) is $\max_{\mathbf{k}} |\Delta_{\mathbf{k}}| = 0.0142t$ for $(\xi_B/a, G) = (1, 3)$ and $n_1 < n < 1 - n_1$ with $n_1 = 0.2$, compared to $\max_{\mathbf{k}} |\Delta_{\mathbf{k}}| = 0.0382t$ for $(\xi_B/a, G) = (1/2, 16.4)$ and $n_1 < n < 1 - n_1$ with $n_1 = 0.23$. The positions (n_1, G) and $(1 - n_1, G)$ of the maxima are indicated by the numbered circles ① for $\xi_B/a = 1$ and ② for $\xi_B/a = 1/2$ in Fig. 4. The reason that one can achieve a larger pairing for smaller ξ_B/a , is that it determines the range of the induced interaction. Since phase separation is mainly driven by long range interactions whereas pairing is mainly driven by the nearest neighbour interactions, a smaller range will suppress pairing less than it suppresses phase separation. As a result of this delicate competition, a small coherence length effectively favours pairing, since it allows a stronger coupling strength before the system phase separates. This shows that our proposed system is very useful for realising a topological superfluid in a lattice, since it allows the tuning of both the strength and the range of the induced interaction.

V. CRITICAL TEMPERATURE OF SUPERFLUID PHASE

Since the Fermi system is 2D, the superfluid phase melts via the BKT mechanism [43–46]. In this section, we calculate the critical temperature T_{BKT} of this transition following the approach of Ref. [47]. The melting is determined by the phase stiffness of the order parameter, which can be calculated from the free energy cost associated with imposing a phase twist on the system. If the overall phase (in addition to the $p_x + ip_y$ phase winding) of the order parameter changes by a small amount $\delta\theta$ between neighbouring sites along the x -direction, the corresponding change in the free energy is

$$F_\theta - F_0 = N \frac{J_x}{2} \delta\theta^2, \quad (15)$$

where J_x is the phase stiffness along the x -direction. Imposing such a linear phase twist on the system is equivalent to using periodic boundary conditions on a system described by the gauge transformed Hamiltonian [48]

$$H_{\text{eff}}(\theta) = e^{-i\frac{\delta\theta}{2} \sum_l x_l/a} H_{\text{eff}} e^{-i\frac{\delta\theta}{2} \sum_l x_l/a}. \quad (16)$$

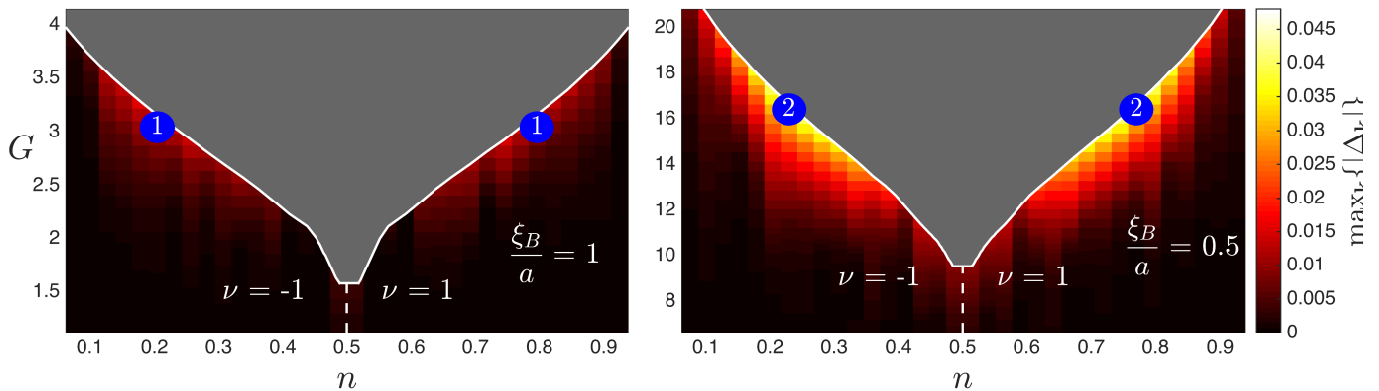


FIG. 4. Zero temperature phase diagram of the fermions as a function of filling fraction n and coupling strength G for $\xi_B/a = 1$ (left) and $\xi_B/a = 1/2$ (right). The color code indicates the maximal magnitude of the gap parameter in the Brillouin zone for a given set of (n, G) . The grey central regions indicate phase separation, and they are centered around half filling. The numbered circles indicates the values (n, G) where the pairing is maximal in the phase diagram. The kinks in the bottom of the phase separation regions are due to the finite resolution of the G -axis. An inspection of the phase separation condition shows that the region boundary must be smooth and have a vanishing derivative at the bottom. The vertical dashed lines indicate a topological phase transition between a phase with Chern number $\nu = -1$ and a phase with $\nu = 1$.

Here, x_l is the x -coordinate of particle l and we gauge transform each particle with half the angle $\delta\theta/2$, since the order parameter $\Delta_{\mathbf{k}}$ involves two particles. From Eq. (15), it is sufficient to calculate the energy shift due to the gauge transformation to second order in $\delta\theta$ to determine the superfluid stiffness. Expanding Eq. (16) to second order in $\delta\theta$, and calculating the corresponding corrections to the energy yields after a lengthy but straightforward calculation [47]

$$J_x = \frac{t}{2N} \sum_{\mathbf{k}} \left[n_{\mathbf{k}} \cos k_x a - \frac{2t}{T} f_{\mathbf{k}} (1 - f_{\mathbf{k}}) \sin^2 k_x a \right] \quad (17)$$

for the superfluid stiffness along the x -direction. Here, $n_{\mathbf{k}} = \langle a_{\mathbf{k}}^\dagger a_{\mathbf{k}} \rangle = |u_{\mathbf{k}}|^2 f_{\mathbf{k}} + |v_{\mathbf{k}}|^2 (1 - f_{\mathbf{k}})$ is the number of fermions with momentum \mathbf{k} and $f_{\mathbf{k}} = (\exp \beta E_{\mathbf{k}} + 1)^{-1}$ is the Fermi function. An equivalent formula holds for the phase stiffness along the y -direction. We find that $J_x = J_y = J$ for $p_x + ip_y$ pairing. The critical temperature for the superfluid phase can now be determined by the BKT condition [43–46]

$$J(T_{\text{BKT}}) = \frac{2}{\pi} T_{\text{BKT}}. \quad (18)$$

In Fig. 5, we plot the calculated phase stiffness $J(T)$ as a function of temperature for the two different parameter sets ① and ② shown in Fig. 4. The critical temperature is from Eq. (18) determined by the crossing of $J(T)$ with the line $2T/\pi$, which is also plotted in Fig. 4. This condition yields the BKT transition temperatures $0.006t$ and $0.017t$ for $(\xi_B/a, n, G) = (1, 0.2, 3)$ and $(\xi_B/a, n, G) = (1/2, 0.23, 16.4)$ respectively. In these calculations, we use that the critical temperature T_c of the BEC typically is much larger than T_{BKT} , so that we can set $T = 0$ when calculating the induced interaction mediated by the BEC. It is straightforward to include non-zero temperature effects on the BEC if necessary.

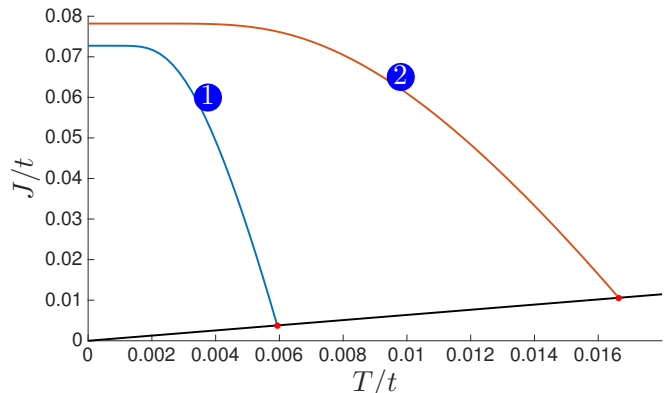


FIG. 5. The phase stiffness given by Eq. (17) as a function of temperature for the two optimal parameter sets ① and ② shown in Fig. 4. The critical temperature is determined when $J(T)$ crosses the line $2T/\pi$, which is also plotted.

VI. DISCUSSION

Despite the fact that we have used the flexibility of the Bose-Fermi system to optimise the interaction for topological pairing, the obtained BKT critical temperatures are still fairly low. As an example, if one takes ${}^6\text{Li}$ atoms in an optical lattice with a wavelength of 1000nm and a lattice depth of $V_0 = 5E_R$, the critical temperature is $T_{\text{BKT}} \simeq 2\text{nK}$ using the parameters corresponding to ② in Fig. 4. The reason for this rather low temperature is that phase separation in the lattice prohibits the use of too strong interaction. One could of course obtain a higher absolute value of the critical temperature by tuning the lattice parameters or by decreasing the coherence length, but here we have chosen to use commonly used experimental values as an example. Another possibility

is to use subwavelength lattices in order to increase the energy scales [49–51]. Finally, it is tempting to suppress phase separation by increasing the temperature, but as we saw from the discussion in connection with Fig. 3, the phase separation instability is unfortunately essentially unaffected by the low temperatures $T \leq T_{\text{BKT}}$, since $T_{\text{BKT}} \ll t$. We note however that the critical temperatures one can obtain in the present system in general are higher than in other lattice proposals, since one can tune both the strength and the range of the interaction. For instance, we find a much lower critical temperature for the system of rotating dipoles in an optical lattice considered in Ref. [28], when the density is the same [52].

Since the Bose-Fermi mixture is a very tunable system compared to other proposals, the fact that we obtain rather low critical temperatures indicates that it will be experimentally challenging to realise a topological superfluid using atoms in an optical lattice. This should be compared with the similar Bose-Fermi system without a lattice, where high critical temperatures can be achieved [31]. The advantage however of using an optical lattice is the available schemes for directly detecting the Majorana edge states. Current experiments with single site resolution [32, 33] could specifically image the edge states using for instance their time-evolution in real

space [53, 54] or RF spectroscopy [34]. Intriguingly, we note that since the two phase separated regions with filling fractions n_1 and $1 - n_1$ have Chern numbers $\nu = -1$ and $\nu = 1$ respectively, there will be topologically robust edge states at the boundary between these two phases.

VII. CONCLUSIONS

In this paper, we have analysed the phase diagram of identical fermions in a 2D square lattice immersed in a 3D BEC. The attractive induced interaction between the fermions mediated by the BEC was shown to give rise to topological $p_x + ip_y$ pairing as well as phase separation. We calculated the phase diagram at zero temperature as a function of the Bose-Fermi coupling strength and the filling fraction. The Bose-Fermi mixture was demonstrated to allow one to maximise topological superfluid pairing by tuning the range of the interaction, so that it favours pairing between nearest neighbour fermions, while long range interaction effects leading to phase separation are suppressed. We then calculated the BKT critical temperature for the superfluid phase, and we finally discussed the prospect for an experimental realisation of a topological superfluid in the present system.

-
- [1] A. Y. Kitaev, *Physics-Uspekhi* **44**, 131 (2001).
- [2] V. Mourik, K. Zuo, S. M. Frolov, S. R. Plissard, E. P. A. M. Bakkers, and L. P. Kouwenhoven, *Science* **336**, 1003 (2012), <http://science.sciencemag.org/content/336/6084/1003.full.pdf>.
- [3] M. T. Deng, C. L. Yu, G. Y. Huang, M. Larsson, P. Caroff, and H. Q. Xu, *Nano Letters* **12**, 6414 (2012), pMID: 23181691, <http://dx.doi.org/10.1021/nl303758w>.
- [4] A. Das, Y. Ronen, Y. Most, Y. Oreg, M. Heiblum, and H. Shtrikman, *Nat Phys* **8**, 887 (2012).
- [5] L. P. Rokhinson, X. Liu, and J. K. Furdyna, *Nat Phys* **8**, 795 (2012).
- [6] A. D. K. Finck, D. J. Van Harlingen, P. K. Mohseni, K. Jung, and X. Li, *Phys. Rev. Lett.* **110**, 126406 (2013).
- [7] S. Nadj-Perge, I. K. Drozdov, J. Li, H. Chen, S. Jeon, J. Seo, A. H. MacDonald, B. A. Bernevig, and A. Yazdani, *Science* **346**, 602 (2014), <http://science.sciencemag.org/content/346/6209/602.full.pdf>.
- [8] S. M. Albrecht, A. P. Higginbotham, M. Madsen, F. Kuemmeth, T. S. Jespersen, J. Nygård, P. Krogstrup, and C. M. Marcus, *Nature* **531**, 206 (2016).
- [9] K. Ishida, H. Mukuda, Y. Kitaoka, K. Asayama, Z. Q. Mao, Y. Mori, and Y. Maeno, *Nature* **396**, 658 (1998).
- [10] K. D. Nelson, Z. Q. Mao, Y. Maeno, and Y. Liu, *Science* **306**, 1151 (2004), <http://science.sciencemag.org/content/306/5699/1151.full.pdf>.
- [11] F. Kidwingira, J. D. Strand, D. J. Van Harlingen, and Y. Maeno, *Science* **314**, 1267 (2006), <http://science.sciencemag.org/content/314/5803/1267.full.pdf>.
- [12] J. Xia, Y. Maeno, P. T. Beyersdorf, M. M. Fejer, and A. Kapitulnik, *Phys. Rev. Lett.* **97**, 167002 (2006).
- [13] V. Gurarie and L. Radzihovsky, *Annals of Physics* **322**, 2 (2007), january Special Issue 2007.
- [14] K. Günter, T. Stöferle, H. Moritz, M. Köhl, and T. Esslinger, *Phys. Rev. Lett.* **95**, 230401 (2005).
- [15] J. P. Gaebler, J. T. Stewart, J. L. Bohn, and D. S. Jin, *Phys. Rev. Lett.* **98**, 200403 (2007).
- [16] J. Levinsen, N. R. Cooper, and V. Gurarie, *Phys. Rev. Lett.* **99**, 210402 (2007).
- [17] M. Jona-Lasinio, L. Pricoupenko, and Y. Castin, *Phys. Rev. A* **77**, 043611 (2008).
- [18] A. Bühler, N. Lang, C. V. Kraus, G. Möller, S. D. Huber, and H. P. Büchler, *Nat Commun* **5** (2014).
- [19] P. Massignan, A. Sanpera, and M. Lewenstein, *Phys. Rev. A* **81**, 031607 (2010).
- [20] L. Mathey, S.-W. Tsai, and A. H. C. Neto, *Phys. Rev. Lett.* **97**, 030601 (2006).
- [21] Y.-J. Wu, J. He, C.-L. Zang, and S.-P. Kou, *Phys. Rev. B* **86**, 085128 (2012).
- [22] C. Zhang, S. Tewari, R. M. Lutchyn, and S. Das Sarma, *Phys. Rev. Lett.* **101**, 160401 (2008).
- [23] M. Sato, Y. Takahashi, and S. Fujimoto, *Phys. Rev. Lett.* **103**, 020401 (2009).
- [24] L. Jiang, T. Kitagawa, J. Alicea, A. R. Akhmerov, D. Pekker, G. Refael, J. I. Cirac, E. Demler, M. D. Lukin, and P. Zoller, *Phys. Rev. Lett.* **106**, 220402 (2011).
- [25] C.-E. Bardyn, M. A. Baranov, E. Rico, A. İmamoğlu, P. Zoller, and S. Diehl, *Phys. Rev. Lett.* **109**, 130402 (2012).
- [26] S. Diehl, E. Rico, M. A. Baranov, and P. Zoller, *Nat Phys* **7**, 971 (2011).
- [27] N. R. Cooper and G. V. Shlyapnikov, *Phys. Rev. Lett.* **103**, 155302 (2009).

- [28] B. Liu and L. Yin, *Phys. Rev. A* **86**, 031603 (2012).
- [29] A. K. Fedorov, S. I. Matveenko, V. I. Yudson, and G. V. Shlyapnikov, *Scientific Reports* **6**, 27448 EP (2016).
- [30] Y. Nishida, *Annals of Physics* **324**, 897 (2009).
- [31] Z. Wu and G. M. Bruun, *ArXiv e-prints* (2016), arXiv:1609.09138 [cond-mat.quant-gas].
- [32] J. F. Sherson, C. Weitenberg, M. Endres, M. Cheneau, I. Bloch, and S. Kuhr, *Nature* **467**, 68 (2010).
- [33] W. S. Bakr, J. I. Gillen, A. Peng, S. Folling, and M. Greiner, *Nature* **462**, 74 (2009).
- [34] S. Nascimbène, *Journal of Physics B: Atomic, Molecular and Optical Physics* **46**, 134005 (2013).
- [35] N. Goldman, J. C. Budich, and P. Zoller, *Nat Phys* **12**, 639 (2016).
- [36] L. Viverit, C. J. Pethick, and H. Smith, *Phys. Rev. A* **61**, 053605 (2000).
- [37] M. J. Bijlsma, B. A. Heringa, and H. T. C. Stoof, *Phys. Rev. A* **61**, 053601 (2000).
- [38] P. W. Anderson and P. Morel, *Phys. Rev.* **123**, 1911 (1961).
- [39] A. Altland and M. R. Zirnbauer, *Phys. Rev. B* **55**, 1142 (1997).
- [40] A. P. Schnyder, S. Ryu, A. Furusaki, and A. W. W. Ludwig, *Phys. Rev. B* **78**, 195125 (2008).
- [41] A. Kitaev, *AIP Conference Proceedings* **1134**, 22 (2009).
- [42] J. Alicea, *Reports on Progress in Physics* **75**, 076501 (2012).
- [43] V. L. Berezinskii, *Soviet Physics JETP* **34**, 610 (1972).
- [44] J. M. Kosterlitz and D. J. Thouless, *Journal of Physics C: Solid State Physics* **6**, 1181 (1973).
- [45] J. M. Kosterlitz, *Journal of Physics C: Solid State Physics* **7**, 1046 (1974).
- [46] P. Chaikin and T. Lubensky, *Principles of Condensed Matter Physics* (Cambridge University Press, 2000).
- [47] A.-L. Gadsbølle and G. M. Bruun, *Phys. Rev. A* **86**, 033623 (2012).
- [48] E. H. Lieb, R. Seiringer, and J. Yngvason, *Phys. Rev. B* **66**, 134529 (2002).
- [49] B. Dubetsky and P. R. Berman, *Phys. Rev. A* **66**, 045402 (2002).
- [50] S. Nascimbene, N. Goldman, N. R. Cooper, and J. Dalibard, *Phys. Rev. Lett.* **115**, 140401 (2015).
- [51] W. Yi, A. J. Daley, G. Pupillo, and P. Zoller, *New Journal of Physics* **10**, 073015 (2008).
- [52] In Ref. [28], the authors present higher critical temperatures for the dipolar system than what we find in the present paper for the Bose-Fermi mixture. However, when using their dipolar interaction in our formalism, we find that they use parameter sets where the system is phase separated.
- [53] N. Goldman, J. Dalibard, A. Dauphin, F. Gerbier, M. Lewenstein, P. Zoller, and I. B. Spielman, *Proceedings of the National Academy of Sciences* **110**, 6736 (2013), <http://www.pnas.org/content/110/17/6736.full.pdf>.
- [54] N. Goldman, G. Jotzu, M. Messer, F. Görg, R. Desbuquois, and T. Esslinger, *Phys. Rev. A* **94**, 043611 (2016).